Systemic antitumor protection by vascular-targeted photodynamic therapy (VTP) involves cellular and humoral immunity

Journal:	*Cancer Immunology Immunotherapy*
Manuscript ID:	CII-08-0074.R1
Manuscript Type:	Original article
Date Submitted by the Author:	n/a
Complete List of Authors:	Preise, Dina; The Weizmann Institute of Science, Biological Regulation Oren, Roni; The Weizmann Institute of Science, Biological Regulation Glinert, Itai; The Weizmann Institute of Science, Biological Regulation Kalchenko, Vyacheslav; The Weizmann Institute of Science, Veterinary Resources Jung, Steffen; The Weizmann Institute of Science, Chemical Immunology Scherz, Avigdor; The Weizmann Institute of Science, Plant Science Salomon, Yoram; The Weizmann Institute of Science, Biological Regulation
Keywords:	bachteriochlorophyll , cancer, immune response, immunotherapy, photodynamic therapy, vascular targeting

Systemic antitumor protection by vascular-targeted photodynamic therapy (VTP) involves cellular and humoral immunity

Dina Preise[1], Roni Oren[1], Itai Glinert[1], Vyacheslav Kalchenko[4], Steffen Jung[3], Avigdor Scherz[2] and Yoram Salomon[1]

[1] Department of Biological Regulation, The Weizmann Institute of Science, Rehovot, Israel
[2] Department of Plant Science, The Weizmann Institute of Science, Rehovot, Israel
[3] Department of Chemical Immunology, The Weizmann Institute of Science, Rehovot, Israel
[4] Department of Veterinary Resources, The Weizmann Institute of Science, Rehovot, Israel

Corresponding author: yoram.salomon@weizmann.ac.il

Keywords: bachteriochlorophyll, cancer, immune response, immunotherapy, photodynamic therapy, vascular targeting.

Abstract

Vascular targeted photodynamic therapy (VTP) takes advantage of intravascular excitation of a photosensitizer (PS) to produce cytotoxic reactive oxygen species (ROS). These ROS are potent mediators of vascular damage inducing rapid local thrombus formation, vascular occlusion and tissue hypoxia. This light-controlled process is used for eradication of solid tumors with Pd-bacteriochlorophyl derivatives (BChl) as PS. Unlike classical photodynamic therapy (PDT), cancer cells are not the primary target for VTP and instead are destroyed by treatment-induced oxygen deprivation. VTP initiates acute local inflammation inside the illuminated area accompanied by massive tumor tissue death. Consequently, in the present study, we addressed the possibility of immune response induction by the treatment that may be considered as an integral part of the mechanism of VTP-mediated tumor eradication. The effect of VTP on the host immune system was investigated using WST11, which is now in Phase II clinical trials for age related macular degeneration and intended to be evaluated for cancer therapy. We found that a functional immune system is essential for successful VTP. Long-lasting systemic antitumor immunity was induced by VTP involving both cellular and humoral components. The antitumor effect was cross-protective against mismatched tumors, suggesting VTP-mediated production of overlapping tumor antigens, possibly from endothelial origin. Based on our findings we suggest that local VTP might be utilized in combination with other anticancer therapies (e.g. immunotherapy) for enhancement of host antitumor immunity in the treatment of both local and disseminated disease.

Introduction

Photodynamic therapy utilizes light-dependent activation of a non-toxic photosensitizer (PS) in the presence of molecular oxygen leading to the formation of cytotoxic reactive oxygen species (ROS). Classical PDT (first and second generation) relies on the selective accumulation of the PS in the tumor cells. The majority of malignant cells are directly ablated by ROS generated upon photosensitization [9, 30]. Vascular targeted PDT (VTP) with Pd-bacteriochlorophyl derivatives (Bchl) differs from classical PDT in many aspects. In contrast to PDT, the intravenously (i.v.) injected Bchl-derived PS do not extravasate and remain constrained in the circulation, thus ROS generated locally upon illumination remain confined to the vascular compartment of the tumor [15, 31, 51], resulting in sever vascular damage and acute blood stasis. As a result, tumor cells become deprived from oxygen and nutrient supply, leading to the elimination of the tumor [27, 36]. The PS used in the present study, WST11, is now in phase II clinical trials for treatment of age-related macular degeneration, a pathological neovascularization of the macula leading to blindness of the patients [45] and is intended to be evaluated for cancer treatment.

In past decades, it was realized that a functional immune system is crucial for long-term survival following PDT. Photosensitization triggers innate immunity with subsequent development of adaptive responses [6, 26, 33]. An acute inflammatory reaction develops during the first hours/days following the treatment. Tumor cells undergoing necrotic or apoptotic death release their antigens into the surrounding inflammatory milieu, encouraging antigen uptake by professional antigen presenting cells (APC), as demonstrated *in vitro* [19], and antigen presentation in a context that strongly promotes formation of specific antitumor immunity. Nevertheless, diverse PS demonstrated different effects on the immune system with some of them being rather immunosuppressive [20, 29, 32]. Additionally, in a study by Henderson *et al* it was demonstrated that the most effective treatment regimen caused a very mild inflammatory response [17]. It therefore seems that the contribution of the immune system to photodynamic tumor ablation is dependent upon the PS and treated tumor, as well as on treatment protocol. Importantly, a recently published case report provided the first evidence of immune system contribution to PDT-mediated tumor eradication in the clinical setup [44]. The patient, treated with chlorine e6-based PDT

for skin angiosarcoma of the upper limbs, showed regression of several untreated tumor foci in both the treated and untreated limbs. Additionally, massive T cell infiltration was found in biopsies of untreated tumors. These exciting observations suggest that the characterization of the immune system's contribution to PDT could harbor potential to improve treatment protocols for the patient's benefit.

In light of the above, it was of interest to investigate the impact of intravascular photosensitization on host immunity based on the different PS, targets and the treatment strategies involved in VTP. Moreover, since hypoxic tumor regions can escape death by PDT/VTP, the involvement of the immune system, if significant, might be important for handling minimal residual disease as well as eradicating distant metastatic foci.

In the course of the present study, we demonstrate that local WST11-VTP induces effective and long-lasting systemic antitumor immunity. Furthermore, in contrast to previous studies [14, 25, 39], the immune protection induced by WST11-VTP was cross-reactive, protecting mice from mismatched tumors. We also show that both humoral and cellular immune arms appear to be involved in VTP-mediated immune response.

Materials and Methods

Cell lines

CT26 mouse colon carcinoma and 4T1 mouse mammary carcinoma cells were cultured in Dulbecco's Modified Eagle's Medium (DMEM) supplemented with 10% fetal calf serum, 2mM glutamine, 100µg/ml penicillin and 100U/ml streptomycin.

Animals

Female, 6-8 weeks old BALB/c, BALB/Nude and NOD/Scid mice were purchased from Harlan Laboratories. Diphtheria toxin (DTx) receptor (DTR) transgenic mice (FVB-Tg Itgax-DTR/GFP 57Lan/J) of BALB/c background were bred in the institute facility [21]. Heterozygous transgenic males were intercrossed with female BALB/c mice. Selection of transgenic offspring was performed by PCR (described under DTR-chimera preparation). All animals were housed and handled in the animal facility according to the guidelines of the Weizmann Institute of Science Animal Care and Use Committee. At the end of the experiments or in the case of animal distress, mice were euthanized by cervical dislocation or by inhaling CO_2.

Photosensitizer

In vitro studies: WST11, a water soluble Bchl derivative (Steba-Biotech, Rehovot, Israel) was dissolved in culture medium at final concentration as indicated in the specific experiments.

In vivo studies: WST11 was dissolved in phosphate buffered saline (PBS) and intravenously (i.v.) injected at doses indicated in the specific experiments.

Light sources

In vitro studies: A home built 755 ± 5 nm LED (light emitting diode) array set at a fluency rate of 2.5mW/cm^2 through a Perspex stage.

In vivo studies: A 4W diode laser (755nm) (CERAMOPTEC, Bonn, Germany) was used at the energy indicated in the specific experiments.

Tumor models

Single cell CT26 and 4T1 suspensions were prepared by scrapping monolayers in exponential growth phase under saline. For local tumor implantation, 2x10^6 washed cells in 50µl PBS were subcutaneously (s.c.) injected to the hind leg of the mice. Tumors were considered suitable for treatment 10-14 days after injection when reaching a diameter of 6-8mm.

For lung metastases assay 2x10^5 of CT26 cells in 200µl PBS were injected i.v. into the mouse tail vein. Two weeks later, mice were sacrificed and lungs were weighed and processed for histological examination. For each experiment the following control groups were used: positive control group-mice received only i.v. injection of tumor cells; naïve control group-mice that were not manipulated.

VTP protocol

Tumor bearing mice were anaesthetized by intra-peritoneal (i.p.) injection of a mixture of ketamine (Rhone Merieux, Lyon, France) and 2% xylazine (Vitamed, Israel) (85 /15%, v/v). The tumor area was illuminated immediately following i.v. injection of WST11 (9mg/kg body weight) (1cmΦ, 30J/cm^2, fluence rate 100mW/cm^2, 5min) [31]. Following illumination, the mice were placed back in the cage. After VTP the animals were injected with 2.5mg/kg finadyne solution (containing 2.5mg/ml flunixin, Schering-Plough, UK) for analgesia.

DTR- Bone Marrow chimera preparation and dendritic cell (DC) depletion protocol

DTR transgenic mice screening was done by PCR using the following primers: DTR1 5'-gcc acc atg aag ctg ctg ccg-3'; DTR2 5'-tca gtg gga att agt cat gcc-3'. DTR

transgenic bone marrow was obtained by flushing tibia, femur and hips with PBS. Ten weeks old BALB/c female mice received a single lethal dose of 800 rad total body irradiation and the following day were reconstituted with DTR transgenic bone marrow (i.v. injection of 4-5x10^6 cells/mouse in 200µl PBS). Mice were allowed eight weeks rest before further use. For local DC depletion, mice were injected peri-tumorally with 200ng DTx (D-2918; Sigma-Aldrich) dissolved in PBS starting 24h before VTP and depletion was maintained for 14 days after VTP by daily injections. For systemic dendritic cell depletion, DTx was injected i.p. (16ng/g body weight) starting 48h before VTP and maintaining the depletion for 14 days by every two days injections. Depletion was verified by flow cytometry.

Histology

Lungs and tumors were excised from euthanized animals and fixed in formaldehyde (4%) or Bouin's fixative at room temperature for 24-48 h. Paraffin embedded sections were prepared and stained with hematoxyline/eosin (H&E) under standard conditions. Slides were examined under light microscope (Nicon Eclipsed E600 equipped with Nikon Digital Camera DMX1200F).

Immunohistochemistry

Slices 4µm thick from tumors fixed with Bouin's fixative were deparaffinized by consecutive immersions in xylene, 100%, 95%, 70%, 50% ethanol and double distilled water. Intrinsic peroxidase activity was inactivated by immersing the slides in 3% H_2O_2 and 1% HCl in methanol/ PBS (1:1). Sections were blocked with 5% bovine serum albumin (BSA) in PBS. For T cell staining, antigen retrieval was done by boiling (10min, 10% efficiency) in 1mM EDTA and then rat α-human CD3 antibodies (Serotec, Raleigh, NC, USA) were applied in PBS containing 1% BSA. After washing in PBS, biotinylated α-rat antibodies were added (Vector Laboratories, Burlingame, CA, USA) and the binding was visualized with avidin-biotin peroxidase complex (Vectastain Elite ABC kit; Vector Laboratories) according to the manufacturer's instructions. For macrophage staining, antigen was retrieved with 0.1% trypsin containing 0.1% $CaCl_2$ in 20mM Tris buffer. Rat α-mouse F4/80 antibodies (Serotec) were applied in 1% BSA and 0.1% triton in PBS. Universal immuno-peroxidase polymer for mouse tissue (Histofine 414311F, Nichirei Corp., Tokyo, Japan) was used according to manufacturer's instructions. For B cell staining, antigen retrieval by boiling (10min, 10% efficiency) with 10mM sodium citrate was

performed. Biotinylated rat α-mouse CD45R antibodies (PharMingen, San Diego, CA USA) were applied and ABC kit was added. Di-amino-benzidine (DAB) reagent (Vector Laboratories) was used for visualization. All slides were counterstained with hematoxylin-Mayer (Finkelman) and examined by light microscopy.

Neutrophil infiltration

Specific neutrophil esterase activity was detected in de-paraffinized slides using naphthol AS-D chloro-acetate esterase kit (Sigma, St. Louis, MO, USA) according to the manufacturer's instructions. Sections were then examined by light microscopy.

Splenocyte isolation

Single-cell suspensions were obtained by passing spleens through a stainless steel grid (mesh size 100 µm). Cells were harvested by centrifugation, depleted of erythrocytes by treatment with lysis solution (155mM NH_4Cl, 10 mM $KHCO_3$, 1 mM EDTA, pH 7.3) and washed with PBS.

Adhesion assay

Single cell suspensions of naïve or stimulated splenocytes were counted and incubated in the dark with vital fluorescent dyes (1,1'-dioctadecyl-3,3,3',3'-tetramethylindocarbocyanine perchlorate (DiI) 5µM or 4-(4-(dihexadecylamino)-styryl-N-methylpyridinium iodide (Di-Asp) 10µM, 30min, RT, Molecular Probes) to enable tracking, then centrifuged in order to remove excess dye and used immediately. Equal numbers of naïve and VTP-sensitized splenocytes were mixed and incubated with cultured tumor cells for 2h at 37°C in 24 well plates. Wells were then washed extensively to remove unbound cells and examined under a fluorescent microscope (Nikon Eclipse TE 2000-U equipped with Nikon LH-M100c-1 camera). Ten images were acquired for each group using respective exitation/emission filter pairs 510-560/590nm and 450-480/505-550nm for DiI and DiO. Area covered by splenocytes was calculated and analyzed with ImageJ software. Statistical analysis was performed using student's t-test.

Cytotoxicity assay

The lytic activity of splenocytes was assessed in a standard 4h cytotoxicity assay. Splenocytes were isolated from naïve mice or mice two weeks after VTP and incubated with cultured CT26 cells at an effector/target ratio of 50:1. After 4h cytotoxicity was tested by colorimetric lactate dehydrogenase (LDH) release assay

using LDH kit (Sigma) according to manufacturer's instructions. The percent of specific lysis was calculated according to formula:

$$\%_{Specific\_Lysis} = [\frac{(Experimental\_Release) - (Spontaneous\_Release)}{(Maximun\_Release) - (Spontaneous\_Release)} * 100]$$

Animal bleeding and serum isolation

Mice were bled peri-orbitally. Whole blood was allowed to clot at room temperature and serum was separated by centrifugation at 4000rpm for 20min. If not used immediately, the serum was stored at -20°C.

IgG binding

CT26 cells were plated in 96-well plates and incubated for 24h. Cells were washed with fresh medium and 50µl of serum diluted 1:5 with assay buffer (Tris-HCl buffer, 50 mMol, pH 7.7, containing BSA (5 g/l), NaCl (9 g/l) and Tween-20 (0.1 ml/l)) added. After 2h incubation at 37°C, cells were washed and blocked with 25µl normal mouse serum (Sigma, St. Louis, MO, USA). Horse α -mouse IgG conjugated to horseradish peroxidase (Vector, Laboratories) was added for one hour. After washing with PBS, color was developed with 3,3',5,5'-tetramethylbenzidine (TMB) solution (Zymed) and read at 650nm on a Victor 1420 multi-label counter (Perkin-Elmer).

Flow cytometry

Mouse lymph nodes and spleens were disaggregated in PBS. For isolation of dendritic cells, tissue was subjected to enzymatic degradation with 1mg/ml collagenase D (Roche) for 30min at 37°C. Single cell suspensions were blocked with rat-α-mouse CD16/32 and stained with appropriate antibodies. Blocking α-CD16/32, FITC-conjugated rat-α-mouse CD4, PE-conjugated hamster-α-mouse CD3 and APC-conjugated rat-α-mouse CD8 antibodies were purchased from eBioscience (San Diego, CA, USA). APC-conjugated hamster-α-mouse CD11c were purchased from BioLegend (San Diego, CA, USA). Single-cell suspensions were prepared in flow cytometry buffer (PBS, 1% FBS, 2 mM EDTA, and 0.05% sodium azide). Cells were analyzed by multicolor flow cytometry using a FACSort cytometer (Becton-Dickinson, Mountain View, CA) and CellQuest software (Becton-Dickinson). A live lymphocyte gate was set according to forward and side scatter parameters. For analysis of T lymphocytes 1-2 $x10^4$ cells were acquired per sample and for dendritic cells 2-5 $x10^5$ cells were acquired.

***In vitro* IFNγ production assay**

Splenocytes were isolated from VTP cured mice (three months after treatment) or naïve BALB/c mice as described above and stimulated with cultured CT26 cells that were previously subjected to a lethal dose of WST11 and light (10μM, 10min illumination). After 2h of stimulation, cytokine secretion was blocked by brefeldin A (3μg/ml, eBioscience) for 4h. Cells were stained for CD4 and CD8 surface markers, permeabilized with permeabilization solution (0.1% saponin, 5% fetal calf serum and 0.1% azide in PBS) and intracellular staining for IFNγ was performed for 30min. Rat-α-mouse INFγ antibodies were purchased from eBioscience. Cells were washed and analyzed by flow cytometry.

Adoptive transfer experiments

Mice cured from CT26 tumors or naïve mice were stimulated by i.p. injection of 10^5 CT26 cells subjected to a lethal dose of WST11 and light. Two days later $CD8^+$ and $CD4^+$ cells were purified from mouse spleens using magnetic beads (BD Bioscience) and immediately injected i.v. to naïve BALB/c mice ($9x10^6$ cells/ mouse) that received lymphodepleting irradiation (300 Rad) a week earlier. Cell purity was determined by flow cytometry and found to be >95% and >91% for $CD8^+$ and $CD4^+$ cells respectively. Two days afterwards adoptive transfer mice were challenged i.v. with live CT26 cells ($2x10^5$ cells/ mouse). Two weeks after challenge mice were sacrificed, the lungs were excised and weighed.

Statistical analysis of tumor infiltration

At least four fields were acquired per section and analyzed with Image Pro Plus or Image J software. The areas covered by neutrophils or $CD3^+$ was measured and compared using student's t-test. At least three mice were tested for each time point.

Results

A functional immune system is necessary for effective eradication of local tumors by WST11-VTP

To investigate the role of adaptive immunity on VTP, we grafted wild type and immuno-deficient mice with mouse CT26 colon carcinoma cells and subjected the developed tumors to WST11-VTP with drug and light doses that gave the highest cure rates as determined in preliminary studies (not shown). We found that while immuno-competent wild type BALB/c mice responded well to the treatment with high cure rates (above 70%), BALB/Nude and NOD/Scid mice that exhibit defects in adaptive

immunity responded very poorly (18.7% and 11%, respectively) (Fig. 1). This demonstrates the necessity of the host immune system for effective VTP. Notably, nude mice lack functional T cells, while Scid mice lack both B and T lymphocytes. However, there was no significant difference in cure rates of the two strains, implying that cell-mediated immunity has a dominant effect over humoral immunity in the acute antitumor action of VTP.

WST11-VTP induces long-lasting systemic heterologous antitumor protection

Next, BALB/c mice bearing s.c. CT26 tumors were subjected to WST11-VTP. Two weeks later the animals were challenged by i.v. injection of viable CT26 cells, and lung metastases development was examined two weeks after challenge. Mice exposed to VTP were found completely protected from metastases (as verified by histological examination), while positive control mice (that received the challenge only) developed multiple tumor foci in the lungs (Fig. 2a, b). This antitumor protection lasted three months post treatment (Fig. 2c) and even up to one year later (data not shown). These results indicate that despite the local nature of the treatment and the fact that tumor cells are not the primary targets, VTP induces systemic and long-lasting antitumor protection.

We also found that when the primary tumor was mouse 4T1 mammary carcinoma, WST11-VTP conferred protection to BALB/c mice against subsequent challenge with CT26 cells as verified two weeks and three months post treatment (Fig. 2d, e). The observed cross-protection phenomenon could potentially be attributed to several mechanisms: (i) antigenic similarity between the tumor types tested, (ii) determinant spreading [18, 37] initiated by VTP-induced oxidative modification of proteins and lipids and (iii) the mounting of specific cellular and/or humoral responses against endothelial cell-derived antigens that might interfere with neo-vascularization upon tumor re-challenge.

An acute inflammatory response is initiated immediately after WST11-VTP

To gain further insight into the protection phenomenon, we performed an in depth characterization of the local VTP response. VTP of s.c. tumors induces acute wounding in the treated site that is resolved within a month after treatment, leaving minimal scaring. We investigated the nature and kinetics of acute inflammatory phase initiated upon vascular photosensitization. A rapid and massive neutrophil infiltration

was observed immediately after illumination. Significant numbers of neutrophils were detected in the tumor rim and the interface between the tumor and the surrounding skin culminating one hour post VTP (Fig. 3). No neutrophils were observed in the tumor core. The number of infiltrating neutrophils then dropped dramatically to non detectable levels 24h post treatment. Additionally, a substantial recruitment of lymphocytes into the tumor was observed 24h post VTP, as confirmed by tumor immuno-staining for the pan T cell marker CD3 (Fig. 4d). Most infiltrated T cells were located in the tumor rim, similarly to the neutrophils. We noted the almost complete absence of $CD3^+$ cells shortly after the illumination (Fig. 4b). Statistical analysis showed significant differences between tumor T cell content one hour post treatment compared to infiltration both before and 24h post VTP ($p<1.5x10^{-7}$ and $p<1.5x10^{-6}$ respectively). Closer examination of the slides under large magnification revealed some $CD3^+$ cells inside and in close proximity to the blood vessels (Fig. 4c) as a first sign of T cell infiltration initiated by VTP. T cell infiltration was almost completely resolved by 48h after treatment ($p<5.7x10^{-6}$ compared to 24h post treatment) (Fig. 4e) with only a few $CD3^+$ cells seen in the areas still containing live tumor cells (Fig. 4f). Possibly, these lymphocytes recognize tumor antigens exposed by VTP and are involved in antitumor cytotoxic lymphocyte (CTL) responses.

Cellular antitumor activity and T cell-mediated immune memory is induced upon WST11-VTP

The results presented in Figs. 2-3 demonstrate rapid recruitment of different immune cells into the treated tumor area. We next decided to test VTP-mediated stimulation of the effector cell activity and formation of immune memory. In an *in vitro* adhesion assay we found that sensitized splenocytes isolated from VTP-treated mice adhered better to cultured tumor cells compared to splenocytes isolated from naïve mice (Fig. 5a). There was a significant difference in adhesion of CT26-sensitized splenocytes to naïve cultured 4T1 cells compared to naïve cultured CT26 cells. However, interestingly, this difference was abolished by photosensitization of tumor cells in culture prior the addition of splenocytes. We hypothesize that the photodynamic treatment produces overlapping tumor antigens by means of oxidative modification and/ or determinant spreading. Importantly this finding is in agreement with the results obtained with these tumor cells *in vivo* (Fig. 2d, e).

We further found that VTP enhanced the cytotoxic activity of sensitized splenocytes compared to naïve splenocytes as judged by a standard *in vitro* cytotoxicity assay (Fig. 5b), confirming the existence of a CTL response. Lymphocytes isolated from mice several months after VTP secreted IFNγ upon re-stimulation with *in vitro* photosensitized tumor cells (Fig. 5c), indicating the generation of a pro-inflammatory Th1 response. Moreover, adoptively transferred $CD8^+$ and $CD4^+$ T cells isolated from surviving mice three months post VTP were able to protect naïve recipients from subsequent challenge with viable cancer cells from the same type (Fig. 5d, e). Together these findings provide strong evidence that VTP induces a T cell-mediated adaptive immune response with formation of effective immune memory.

VTP-induced stimulation of humoral immunity

Recent studies demonstrated that *in vivo* antitumor antibody-dependent cell cytotoxicity (ADCC) is one of the mechanisms of antitumor immunity [22, 41, 42]. To investigate the involvement of humoral immune responses in VTP-mediated antitumor action we utilized several approaches. Immuno-blotting of untreated or VTP pre-treated tumor lysates with serum from naïve or treated mice revealed several changes in the pattern of antigens recognized by the serum IgGs. For example, new bands were recognized by serum from treated animals in the lysate of untreated tumor cells indicating production of novel antibodies against existing antigens (Fig. 6a-*a*). New bands in the lysates of treated tumors blotted with naïve mouse serum indicate formation of new antigenic epitopes or VTP-mediated exposure of those previously hidden (Fig. 6a-*b*). Additionally, some antigens were probably oxidatively modified preventing immune recognition as was demonstrated by bands that disappeared 24h post VTP (Fig. 6a-*c*). Histological examination of VTP-treated tumors revealed that one hour after illumination only a few B cells were found within the tumor, most of them inside or in close proximity to blood vessels similarly to T cells, indicating B cell recruitment initiated by VTP (Fig. 6b). A marked B cell infiltration was observed 24h after treatment in the tumor rim with some cells distributed throughout the tumor and in the connective tissue between the skin and the tumor. Some of these cells could still be seen 48h after VTP. Increased serum IgG titers were detected one week after VTP as judged by *in vitro* binding to respective tumor cells (Fig. 6c) compared with serum from naïve and untreated tumor-bearing mice. It was therefore of interest to verify the contribution of these humoral components to the tumor eradication process.

Transfer of serum from mice cured from CT26 tumors protected the naïve recipients from subsequent challenge with live CT26 cells (Fig. 6d). To the best of our knowledge, this is the first demonstration that humoral immunity contributes to VTP-mediated antitumor protection.

Dendritic cells are necessary for VTP-mediated eradication of local tumors

Next we investigated the contribution of dendritic cells to the VTP triggered immune response. Lethally irradiated BALB/c mice were reconstituted with bone marrow of mice expressing a diphtheria toxin (DTx) receptor transgene under the CD11c promoter, enabling selective depletion of dendritic cells upon DTx injection [21, 40] (Fig 7a). In this model only transgenic cells are sensitive to DTx-mediated depletion, while no effect was observed upon DTx injection to the wild type mice. After a two month recovery period, the mice were s.c. implanted with CT26 tumors and subjected to WST11-VTP with or without dendritic cell depletion. Two depletion protocols were tested: (i) local depletion by peri-tumoral DTx injections starting 24h before the treatment and continuing with daily injections for 14 consecutive days and (ii) systemic depletion by i.p. injection of DTx starting 48h before VTP followed by injections every two days for 14 days post treatment. We found that both protocols resulted in significantly higher tumor recurrence rates compared to VTP alone (Fig. 7b, c). No effect on tumor growth was observed in mice that received DTx without VTP and the animals were sacrificed shortly thereafter due to tumor progression. This is the first direct evidence supporting dendritic cell contribution to tumor destruction by VTP.

Discussion

There is increasing recognition that the immune system can effectively contribute to the eradication of solid tumors. The major disadvantage of chemo- and radiotherapy is that these modalities suppress host immunity preventing its beneficial consequence on the treatment outcome. Therefore, any anticancer modality that preserves or even enhances host immune responses will be particularly valuable in the fight against this fatal disease. Vascular-targeted photodynamic therapy (VTP) relies on intravascular photosensitization without direct ablation of tumor cells [15, 31, 36]. In previous reports, we demonstrated the benefit of targeting the non-malignant tumor

vasculature, by effective eradication of drug-resistant tumors [36]. In the present study we tested the hypothesis that an acute VTP-mediated inflammatory response, together with the rapid necrotic death of a large tumor mass, might provide a perfect milieu for effective antitumor sensitization of the host immune system. The results presented here provide first evidence for immune system involvement in systemic antitumor protection induced by VTP with the Bchl derivative WST11. Data available in the current literature relates to first generation photosensitizers, whose action is based on selective PS accumulation within tumor cells. It was shown in various experimental settings that the immune effect of PDT is dependent on multiple factors such as photosensitizer type, treatment regimen and specific tumor model and can vary from effective pro-inflammatory responses to systemic immunosuppression [10, 11, 13, 25, 50].

In our study we found that mice lacking a functional immune system are less responsive to WST11-VTP than immunocompetent BALB/c mice (Fig. 1), demonstrating that an immune reaction is crucial for successful eradication of local tumors by VTP, similarly to other PDT protocols [13, 23, 24]. Moreover, VTP of local mouse CT26 colon tumors grown in BALB/c mice induced systemic protection against a second tumor challenge in cured mice (Fig. 2a-c). Surprisingly, in contrast to PDT with hematoporphyrin-based and other photosensitizers that always induced tumor specific immunity [14, 25, 39], protection induced by WST11-VTP was found to be non-tumor specific. Namely, mice cured from local mouse 4T1 mammary tumors resisted the challenge with CT26 cells (Fig. 2d, e). We hypothesize that several mechanisms can be responsible for this cross-protection phenomenon. First, it was previously shown that some tumors share antigenic epitopes that may result in cross-reactivity [38]. Second, cross-protection could be attributed to the determinant spreading phenomenon in which T cell responses, initiated by a single antigenic epitope, may evolve into multi-epitopic responses [5, 37]. In case of VTP, the large amount of potentially antigenic molecules that is released from dying tumor cells can provide a vast reservoir of such epitopes. Finally, the most interesting possibility relies on the antivascular nature of our treatment modality. It was shown that tumor vessels express unique antigens that distinguish it from the normal vasculature [43, 46]. Moreover, it was demonstrated that targeting such antigens, for example vimentin, with specific antibodies inhibited angiogenesis and markedly reduced tumor growth. This was also accompanied by reduced microvessel density, implying that the

antiangiogenic character of the treatment is responsible for the observed effect. In another study vaccination with tumor endothelial marker 8 (TEM8) combined with xenogeneic tumor antigens induced effective immunity against tumor challenge [12]. In this study TEM8 had no activity as a single agent but significantly enhanced the antitumor immunity for the second antigen, demonstrating effect of adjuvant rather than immunologic target. Since in VTP the photosensitization process is confined to the vascular compartment of the tumor, it is likely that photodamaged endothelial cells may provide an additional significant source of such specific antigens that could augment immune responses. When modified by VTP-induced ROS, some of those putative antigens might even become sufficiently immunogenic to be recognized by the immune system. These antigens are host derived and as such are expected to be at least in part shared by different tumors as documented previously [43], forming a basis for mismatched tumor protection. The specific adaptive immune memory induced against these antigens upon VTP may inhibit the development of new tumors by interfering with their angiogenesis. Several studies report that oxidative modifications such as nitration of proteins [16, 34, 35] or formation of aldehyde adducts of phospholipids and lipoproteins [49] are capable of breaking immune tolerance to the modified entities. It was even demonstrated that, in case of 4-hydroxynonenal (HNE) adduction, the induced immune cells also mediated responses against parental unmodified proteins [48], which is particularly important for eradication of distant metastases. We found previously that VTP with BChl derivatives induces lipid peroxidation with formation of HNE adducts [27, 36], as well as protein nitration (Gal, Preise unpublished). Therefore, these VTP-induced modifications could be partly responsible for treatment-enhanced tumor immunogenicity. It is known that classical PDT also induces different degrees of vascular damage (depending on PS and drug-to-light interval) [10]. Nevertheless, the highest sensitizer concentration is found in the tumor cells and not in the vasculature, thus the contribution of vasculature-related factors on immune stimulation is probably minor and not expected to have a significant impact on the final outcome.

Acute inflammatory reactions manifested by neutrophil tumor infiltration started immediately upon treatment completion, culminating 1h post VTP with a drop in cell numbers within the tumor area (Fig. 3). These findings are in line with other reports [24, 28] but the infiltration kinetics are faster than reported by those authors that found maximal neutrophil recruitment 24h post treatment. In the wound healing

process, the neutrophils progressively accumulate in the damaged site for a few days after the injury (maximal infiltration around 12-24h post injury and then their numbers progressively decline) [2, 8]. The consequence of such rapid neutrophil clearance from VTP-treated area might be a prolonged exposure of tumor-derived antigens (which are not removed fast enough) to immune cells participating in activation and propagation of adaptive immune response (like dendritic cells that cross-prime tumor specific T cells) leading to the formation of effective antitumor memory.

T cells are known mediators of adaptive immune responses. We found that existing T cells in the tumor before treatment (Fig. 4a) could not be detected already one hour post VTP (Fig. 4b). In agreement with data showing that immune cells are highly susceptible to direct photodynamic action [4], these T cells are probably destroyed by the treatment. This might be beneficial to the final treatment outcome as multiple studies show that these tumor infiltrating lymphocytes suppress antitumor functions, many of them are actually regulatory T cells inhibiting pro-inflammatory immune responses [1]. By removing this tumor-imposed suppression, VTP may open an opportunity for effective pro-inflammatory Th1 immune polarization by lymphocytes recruited upon photosensitization. Such newly infiltrating T cells can be seen at the proximity of tumor feeding blood vessels shortly after VTP (Fig. 4c). Taken together, the recruitment of neutrophils and T lymphocytes into the illuminated area denote a strong and rapid inflammatory reaction, initiated shortly after VTP and practically resolved several days after treatment. This is much faster than in wound- or bacteria-induced inflammation, where infiltrate accumulates for several days and stays for up to two weeks [8]. The reason could be the rapid occlusion of tumor feeding blood vessels, precluding further accumulation of immune cells.

It is worth mentioning that two papers reported that PDT protocols inducing maximal inflammatory response are actually less effective in local tumor eradication [17, 28]. In the study by Kousis *et al*, a less inflammatory regimen was highly efficient in inhibiting the tumor growth, but did not induce durable immune responses [28]. Consequently, the authors proposed combination of inflammation-inducing PDT protocol with additional agents enabling efficient control of the treated tumor. In contrast, in our work, the VTP protocol applied induced the highest cure rates in our experimental set up and provided long-lasting systemic protection from repetitive tumor challenges.

The role of humoral immunity in PDT/VTP was only occasionally addressed. PDT with meta-tetra(hydroxyphenyl)bacteriochlorin (mTHPBC) of rat CC531 colon adenocarcinoma tumors failed to induce anti-CC531 antibodies [47]. Chen *et al* reported some new bands in western blots of tumors probed with sera from rats cured by Photofrin-PDT combined with the immune-adjuvant glycated chitosan [7] suggesting that combined treatment resulted in development of specific antitumor antibodies. In our study we also found different protein patterns when tumors were probed with sera from naïve or successively cured mice (Fig. 6a). The comparison between untreated tumors and tumors 24h after VTP demonstrates that there are antigens that normally escape the immune system but become exposed upon treatment, as they were recognized by antibodies from naïve mice. Additionally, serum obtained from treated animals contained novel antibodies recognizing antigens in the untreated tumor, suggesting that VTP converted these antigens to more immunogenic. Overall IgG binding to cultured tumor cells revealed increased titers in the treated animals (Fig. 6c). Taken together these findings suggest that VTP enables more effective immune probing of the tumor cells by exposing tumor antigens to immune cells. Our results obtained from the serum transfers provide first evidence that humoral immunity is sufficiently stimulated by VTP to induce antitumor protection in naïve mice (Fig. 6). The remaining question is concerning the nature of soluble factors that mediate the observed effect and the exact mechanism by which tumor rejection is achieved. In the preliminary experiment we found that serum transfer into lympho-depleted mice failed to protect the recipients from subsequent tumor challenge (unpublished data) suggesting ADCC is responsible for the observed protection.

Exposure of dendritic cells to photosensitized tumor cells in culture reportedly induces their phenotypical and functional maturation [14]. Dendritic cells represent a crucial link between innate and adaptive immunity [3]. As professional APC they are unrivaled in potential to induce primary immune responses, thus permitting the establishment of immunological memory [3]. Following tissue damage and upon antigen uptake, dendritic cells migrate to the regional lymph nodes and initiate specific adaptive immune responses. Consequently, the combination of PDT with ATX-S10 Na(II), a hydrophilic chlorin photosensitizer, [39] and Photofrin [19] with intra-tumoral injection of immature dendritic cells was shown to be beneficial for tumor eradication. We utilized a transgenic mouse model in which selective depletion

of dendritic cells can be achieved (Fig. 7a) [21]. Using these mice we demonstrate that local and systemic depletion of dendritic cells during VTP and for short period after the treatment greatly reduces VTP effectiveness (Fig 7b, c). This suggests that these cells actively participate in the acute phase of VTP-mediated stimulation of immune responses affecting the final treatment outcome.

Taken together, the observations presented in this study demonstrate that the host immune response elicited by tumor WST11-VTP is an integral component of the therapeutic effect of this modality. WST11-VTP induces long-lasting highly efficient antitumor protection. VTP activates cellular and humoral immune arms and possibly the final outcome is achieved by the contribution of both. Further research is needed in order to better understand the mechanism of VTP-induced antitumor immunity with emphasis on the nature of antigens that are involved and immune cells that participate in the process. This information may enable improvement of current anticancer immunotherapy protocols. Moreover, novel approaches combining additional immune stimulation with VTP may further augment the efficiency of the treatment of local tumors and possibly to provide an adjuvant effect in the treatment of disseminated disease.

AKNOWLEDGEMENTS

Y.S. and A.S are the incumbents of the Tillie and Charles Lubin Professorial Chair in Biochemical Endocrinology, and the Robert and Yaddele Sklare Professorial Chair in Biochemistry respectively. S.J. is the incumbent of the Pauline Recanati Career Development Chair. D.P. in partial fulfillment of her PhD Thesis requirements at the Feinberg graduate school of the Weizmann Institute of Science. The authors wish to thank Prof. L. Eisenbach and Dr. E. Tzehoval for valuable discussions and technical help, to Dr. Ori Brener for histopathology work, to Ester Shai, for her technical help. Study supported by STEBA-BIOTECH (France).

REFERENCES

1. Adam JK, Odhav B, Bhoola KD (2003) Immune responses in cancer. Pharmacol Ther 99:113-132
2. Agaiby AD, Dyson M (1999) Immuno-inflammatory cell dynamics during cutaneous wound healing. J Anat 195 (Pt 4):531-542

3. Banchereau J, Briere F, Caux C, Davoust J, Lebecque S, Liu YJ, Pulendran B, Palucka K (2000) Immunobiology of dendritic cells. Annu Rev Immunol 18:767-811
4. Boumedine RS, Roy DC (2005) Elimination of alloreactive T cells using photodynamic therapy. Cytotherapy 7:134-143
5. Butterfield LH, Ribas A, Dissette VB, Amarnani SN, Vu HT, Oseguera D, Wang HJ, Elashoff RM, McBride WH, Mukherji B, Cochran AJ, Glaspy JA, Economou JS (2003) Determinant spreading associated with clinical response in dendritic cell-based immunotherapy for malignant melanoma. Clin Cancer Res 9:998-1008
6. Castano AP, Mroz P, Hamblin MR (2006) Photodynamic therapy and anti-tumour immunity. Nat Rev Cancer 6:535-545
7. Chen WR, Huang Z, Korbelik M, Nordquist RE, Liu H (2006) Photoimmunotherapy for cancer treatment. J Environ Pathol Toxicol Oncol 25:281-291
8. Diegelmann RF, Evans MC (2004) Wound healing: an overview of acute, fibrotic and delayed healing. Front Biosci 9:283-289
9. Dolmans DE, Fukumura D, Jain RK (2003) Photodynamic therapy for cancer. Nat Rev Cancer 3:380-387
10. Dougherty TJ, Gomer CJ, Henderson BW, Jori G, Kessel D, Korbelik M, Moan J, Peng Q (1998) Photodynamic therapy. J Natl Cancer Inst 90:889-905
11. Elmets CA, Bowen KD (1986) Immunological suppression in mice treated with hematoporphyrin derivative photoradiation. Cancer Res 46:1608-1611
12. Felicetti P, Mennecozzi M, Barucca A, Montgomery S, Orlandi F, Manova K, Houghton AN, Gregor PD, Concetti A, Venanzi FM (2007) Tumor endothelial marker 8 enhances tumor immunity in conjunction with immunization against differentiation Ag. Cytotherapy 9:23-34
13. Gollnick SO, Owczarczak B, Maier P (2006) Photodynamic therapy and anti-tumor immunity. Lasers Surg Med 38:509-515
14. Gollnick SO, Vaughan L, Henderson BW (2002) Generation of effective antitumor vaccines using photodynamic therapy. Cancer Res 62:1604-1608
15. Gross S, Gilead A, Scherz A, Neeman M, Salomon Y (2003) Monitoring photodynamic therapy of solid tumors online by BOLD-contrast MRI. Nat Med 9:1327-1331
16. Habib Moinuddin S, Ali R (2005) Peroxinitrite modified DNA: a better antigen for systemic lupus erythematosus anti-DNA autoantibodies. Biotechnol Appl Biochem:
17. Henderson BW, Gollnick SO, Snyder JW, Busch TM, Kousis PC, Cheney RT, Morgan J (2004) Choice of oxygen-conserving treatment regimen determines the inflammatory response and outcome of photodynamic therapy of tumors. Cancer Res 64:2120-2126
18. Houghton AN, Guevara-Patino JA (2004) Immune recognition of self in immunity against cancer. J Clin Invest 114:468-471
19. Jalili A, Makowski M, Switaj T, Nowis D, Wilczynski GM, Wilczek E, Chorazy-Massalska M, Radzikowska A, Maslinski W, Bialy L, Sienko J, Sieron A, Adamek M, Basak G, Mroz P, Krasnodebski IW, Jakobisiak M, Golab J (2004) Effective photoimmunotherapy of murine colon carcinoma induced by the combination of photodynamic therapy and dendritic cells. Clin Cancer Res 10:4498-4508

20. Jolles CJ, Ott MJ, Straight RC, Lynch DH (1988) Systemic immunosuppression induced by peritoneal photodynamic therapy. Am J Obstet Gynecol 158:1446-1453
21. Jung S, Unutmaz D, Wong P, Sano G, De los Santos K, Sparwasser T, Wu S, Vuthoori S, Ko K, Zavala F, Pamer EG, Littman DR, Lang RA (2002) In vivo depletion of CD11c(+) dendritic cells abrogates priming of CD8(+) T cells by exogenous cell-associated antigens. Immunity 17:211-220
22. Kasprzyk PG, Song SU, Di Fiore PP, King CR (1992) Therapy of an animal model of human gastric cancer using a combination of anti-erbB-2 monoclonal antibodies. Cancer Res 52:2771-2776
23. Korbelik M (2006) PDT-associated host response and its role in the therapy outcome. Lasers Surg Med 38:500-508
24. Korbelik M, Cecic I (1999) Contribution of myeloid and lymphoid host cells to the curative outcome of mouse sarcoma treatment by photodynamic therapy. Cancer Lett 137:91-98
25. Korbelik M, Dougherty GJ (1999) Photodynamic therapy-mediated immune response against subcutaneous mouse tumors. Cancer Res 59:1941-1946
26. Korbelik M, Sun J, Cecic I (2005) Photodynamic therapy-induced cell surface expression and release of heat shock proteins: relevance for tumor response. Cancer Res 65:1018-1026
27. Koudinova NV, Pinthus JH, Brandis A, Brenner O, Bendel P, Ramon J, Eshhar Z, Scherz A, Salomon Y (2003) Photodynamic therapy with Pd-Bacteriopheophorbide (TOOKAD): successful in vivo treatment of human prostatic small cell carcinoma xenografts. Int J Cancer 104:782-789
28. Kousis PC, Henderson BW, Maier PG, Gollnick SO (2007) Photodynamic Therapy Enhancement of Antitumor Immunity Is Regulated by Neutrophils. Cancer Res 67:10501-10510
29. Lynch DH, Haddad S, King VJ, Ott MJ, Straight RC, Jolles CJ (1989) Systemic immunosuppression induced by photodynamic therapy (PDT) is adoptively transferred by macrophages. Photochem Photobiol 49:453-458
30. Macdonald IJ, Dougherty GJ (2001) Basic principles of photodynamic therapy. J of Porphyrins and Phthalocyanines 5:105-129
31. Mazor O, Brandis A, Plaks V, Neumark E, Rosenbach-Belkin V, Salomon Y, Scherz A (2005) WST11, a novel water-soluble bacteriochlorophyll derivative; cellular uptake, pharmacokinetics, biodistribution and vascular-targeted photodynamic activity using melanoma tumors as a model. Photochem Photobiol 81:342-351
32. Musser DA, Fiel RJ (1991) Cutaneous photosensitizing and immunosuppressive effects of a series of tumor localizing porphyrins. Photochem Photobiol 53:119-123
33. Nowis D (2005) The influence of photodynamic therapy on the immune response. Photodiagnosis and Photodynamic Therapy 2:283-298
34. Ohmori H, Kanayama N (2005) Immunogenicity of an inflammation-associated product, tyrosine nitrated self-proteins. Autoimmun Rev 4:224-229
35. Ohmori H, Oka M, Nishikawa Y, Shigemitsu H, Takeuchi M, Magari M, Kanayama N (2005) Immunogenicity of autologous IgG bearing the inflammation-associated marker 3-nitrotyrosine. Immunol Lett 96:47-54
36. Preise D, Mazor O, Koudinova N, Liscovitch M, Scherz A, Salomon Y (2003) Bypass of tumor drug resistance by antivascular therapy. Neoplasia 5:475-480

37. Ribas A, Timmerman JM, Butterfield LH, Economou JS (2003) Determinant spreading and tumor responses after peptide-based cancer immunotherapy. Trends Immunol 24:58-61
38. Rodeberg DA, Erskine C, Celis E (2007) In vitro induction of immune responses to shared tumor-associated antigens in rhabdomyosarcoma. J Pediatr Surg 42:1396-1402
39. Saji H, Song W, Furumoto K, Kato H, Engleman EG (2006) Systemic antitumor effect of intratumoral injection of dendritic cells in combination with local photodynamic therapy. Clin Cancer Res 12:2568-2574
40. Sapoznikov A, Fischer JA, Zaft T, Krauthgamer R, Dzionek A, Jung S (2007) Organ-dependent in vivo priming of naive CD4+, but not CD8+, T cells by plasmacytoid dendritic cells. J Exp Med 204:1923-1933
41. Schreiber GJ, Hellstrom KE, Hellstrom I (1992) An unmodified anticarcinoma antibody, BR96, localizes to and inhibits the outgrowth of human tumors in nude mice. Cancer Res 52:3262-3266
42. Sondel PM, Hank JA (2001) Antibody-directed, effector cell-mediated tumor destruction. Hematol Oncol Clin North Am 15:703-721
43. St Croix B, Rago C, Velculescu V, Traverso G, Romans KE, Montgomery E, Lal A, Riggins GJ, Lengauer C, Vogelstein B, Kinzler KW (2000) Genes expressed in human tumor endothelium. Science 289:1197-1202
44. Thong PS, Ong KW, Goh NS, Kho KW, Manivasager V, Bhuvaneswari R, Olivo M, Soo KC (2007) Photodynamic-therapy-activated immune response against distant untreated tumours in recurrent angiosarcoma. Lancet Oncol 8:950-952
45. Valamanesh F, Berdugo M, Bejjani RA, Savoldelli M, Jeanny JC, Brun PH, Blanc D, Ben-Ezra D, Behar-Cohen F (2004) Reduced collateral effect of photodynamic therapy (PDT) using a new water soluble photosensitizing agent. Invesr Ophthalmol Vis Sci 45:
46. van Beijnum JR, Dings RP, van der Linden E, Zwaans BM, Ramaekers FC, Mayo KH, Griffioen AW (2006) Gene expression of tumor angiogenesis dissected: specific targeting of colon cancer angiogenic vasculature. Blood 108:2339-2348
47. van Duijnhoven FH, Tollenaar RA, Terpstra OT, Kuppen PJ (2005) Locoregional therapies of liver metastases in a rat CC531 coloncarcinoma model results in increased resistance to tumour rechallenge. Clin Exp Metastasis 22:247-253
48. Wuttge DM, Bruzelius M, Stemme S (1999) T-cell recognition of lipid peroxidation products breaks tolerance to self proteins. Immunology 98:273-279
49. Yla-Herttuala S, Palinski W, Butler SW, Picard S, Steinberg D, Witztum JL (1994) Rabbit and human atherosclerotic lesions contain IgG that recognizes epitopes of oxidized LDL. Arterioscler Thromb 14:32-40
50. Yusuf N, Katiyar SK, Elmets CA (2008) The Immunosuppressive Effects of Phthalocyanine Photodynamic Therapy in Mice Are Mediated by CD4(+) and CD8(+) T Cells and Can Be Adoptively Transferred to Naive Recipients. Photochem Photobiol:
51. Zilberstein J, Schreiber S, Bloemers MC, Bendel P, Neeman M, Schechtman E, Kohen F, Scherz A, Salomon Y (2001) Antivascular treatment of solid melanoma tumors with bacteriochlorophyll-serine-based photodynamic therapy. Photochem Photobiol 73:257-266

FIGURE LEGENDS

Figure 1. Effect of host immune system on WST11-VTP efficacy. Three mouse strains with normal (BALB/c; squares, n=11), T cell deficient (BALB/Nude; triangles, n=16) or T and B cell deficient (NOD/Scid; circles, n=18) immune system and bearing CT26 s.c. tumors were subjected to WST11-VTP and monitored for tumor response. * P<0.004 by students t test.

Figure 2. WST11-VTP induced systemic anti-tumor protection. BALB/c mice bearing s.c CT26 tumors were subjected to VTP and challenged i.v. with viable CT26 cells. Lungs were excised two weeks after challenge and weighed. (**a**) Lung micrographs and respective histological images. (**b**) Homologous protection two weeks and (**c**) Three months after VTP. (**d**) Cross-protection two weeks and (**e**) Three months after VTP. Positive control- naïve age-matched mice i.v. injected with CT26 cells. Representatives of 2-3 experiments are shown. * P<0.008 by students t test.

Figure 3. Neutrophil infiltration into the s.c. CT26 tumors following WST11-VTP. Formaldehyde fixed tumors were stained for specific naphthol AS-D chloroacetate esterase activity. Analysis was done using Image Pro Plus software. Neutrophils are stained in purple. Three mice were used for each time point. One representative experiment is shown. Each bar represents percent of area covered by neutrophils of 4-6 sequential fields taken from one slide normalized to total tumor area (mean ±SE), N=3.

Figure 4. $CD3^+$ lymphocytes infiltration into the CT26 s.c. tumors following WST11-VTP. Tumors were excised at various times after the treatment, fixed in Bouin's fixative and paraffin-embedded. Slices were stained with α-mouse $CD3^+$ antibodies. $CD3^+$ lymphocytes are stained in brown. (**a**) Untreated tumor (**b**) One hour after VTP (**c**) Magnification of the square from B (**d**) 24h after VTP. (**e**) 48h after VTP (**f**) Magnification of the square from E. T-tumor; BV-blood vessel; N-necrotic area; arrows denote $CD3^+$ cells. Each bar represents percent of area covered by $CD3^+$ of 4-6 sequential fields taken from one section normalized to total tumor area (mean ±SE), n=3.

Figure 5. Cellular immune responses induced by WST11-VTP. (**a**) Adhesion of VTP-sensitized or naïve splenocytes to cultured tumor cells. Splenocytes were stained with DiI or DiO vital dyes and incubated with untreated or photodynamically pre-treated cultured CT26 or 4T1 cells. Adhesion was assessed by fluorescent microscope. 10 images were acquired for each group using appropriate filter sets and area covered by splenocytes was calculated. P<0.005; (**b**) VTP-induced splenocyte cytotoxicity. Splenocytes were incubated with cultured CT26 cells. Specific cytotoxicity was measured by LDH release according to formula: % specific lysis= (experimental release-spontaneous release)/ (maximum release-spontaneous release)*100. Experiments were performed in triplicates. (**c**) INFγ secretion by splenic T cells isolated from naïve or cured mice upon *in vitro* re-stimulation with VTP-treated CT26 cells. (**d**) $CD8^+$ cells adoptive transfer; P<0.03 (**e**) $CD4^+$ cells adoptive transfer; P<0.005.Cells were isolated from naïve or cured mice and i.v. injected to lymphodepleted naïve recipients that were subsequently challenged i.v. with $2x10^5$ live CT26 cells and lung metastases development was assessed by lung weighing two weeks after challenge. Control mice were injected with PBS; representatives of 2-3 experiments are shown. (**f**) Verification of lymphodepletion in BALB/c mice. Depletion was tested in peripheral blood of the mice irradiated with 300Rad a week earlier. Blood was collected in the presence of anticoagulant, cells separated by gradient centrifugation and stained for flow cytometry analysis.

Figure 6. Humoral responses induced by WST11-VTP. (**a**) Sera from naïve mice or mice one or two weeks after CT26 tumor VTP was blotted against homogenates of untreated CT26 tumor or tumor isolated 24h after VTP; a- new Abs formed after VTP, b- new or hidden Ag

exposed by VTP, c- Ag that disappeared after treatment. (**b**) $CD45R^+$ cell infiltration into the CT26 s.c. tumors. Positive cells are stained in brown. T-tumor; BV-blood vessel; arrows denote $CD45R^+$ cells. N=3. (**c**) Serum IgG binding to cultured CT26 cells. Serum was obtained from naïve mice and mice bearing CT26 s.c. tumors before and one week after VTP and applied on cultured CT26 cells. Binding was detected with HRP-conjugated anti-mouse IgG antibodies. N=3. (**d**) Serum transfer. Serum from naïve and cured mice was injected i.v. (500µl/mouse) to naïve mice that were subsequently challenged with $2x10^5$ live CT26 cells and lung metastases development was assessed by lung weighing two weeks after challenge. A representative of two experiments is shown. P<0.001

Figure 7. Effect of DCs depletion on WST11-VTP. DTR bone marrow chimera mice bearing CT26 s.c. tumors were depleted from DCs and subjected to WST11-VTP. (**a**) Effect of systemic DTx injection on splenic DC population (**b**) Local DC depletion was initiated by peri-tumoral DTx injection 24h before VTP and maintained by daily injections for 14 days. P< 0.04 (**c**) Systemic DC depletion was initiated by i.p. DTx injection 48h before VTP and maintained by every two days injection for 14 days. P< 0.004 Group received VTP only (squares, n=17), group received VTP with depletion (triangles, local n=28; systemic n=11), group received DTx only (circles, local n=6; systemic n=5).

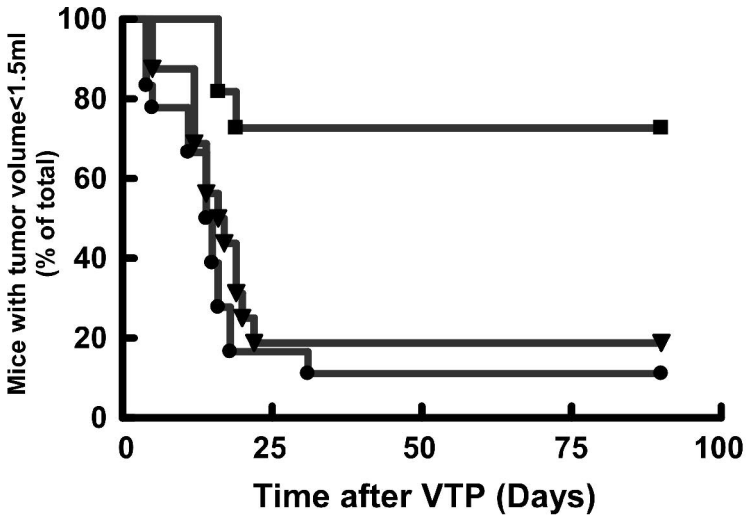

Figure 1
135x85mm (600 x 600 DPI)

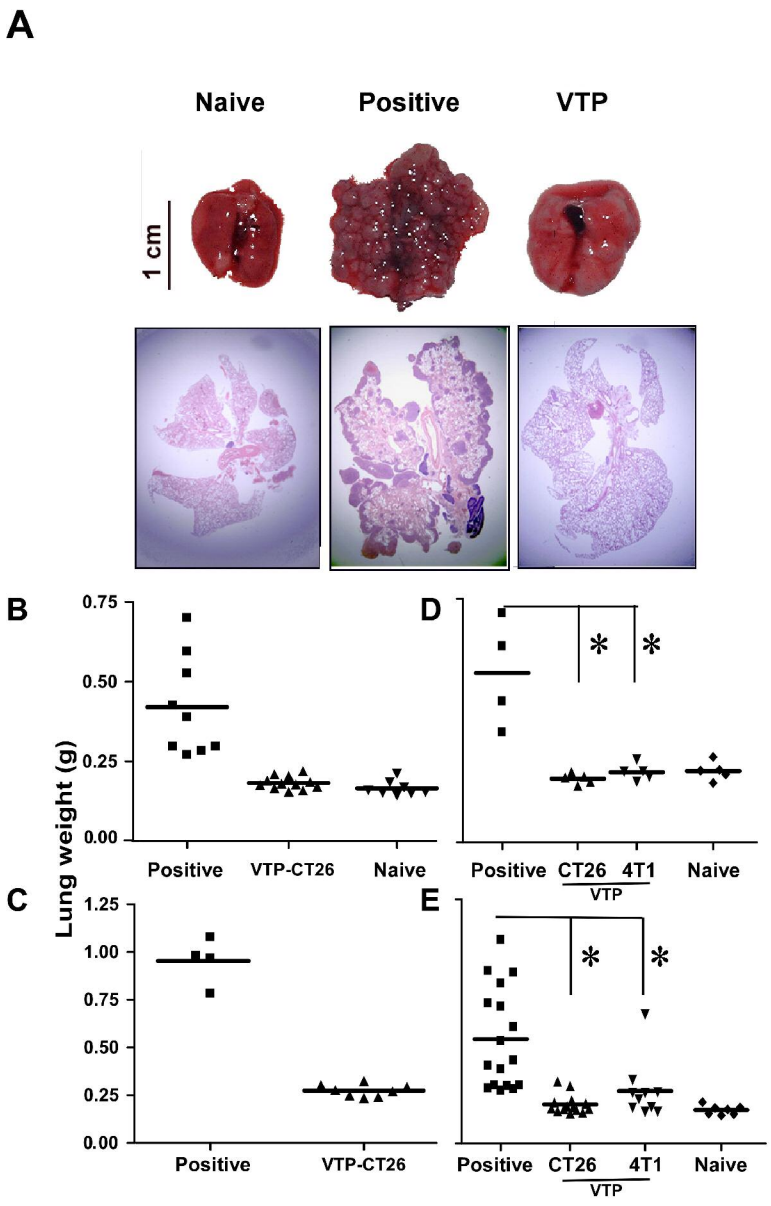

Figure 2
97x152mm (600 x 600 DPI)

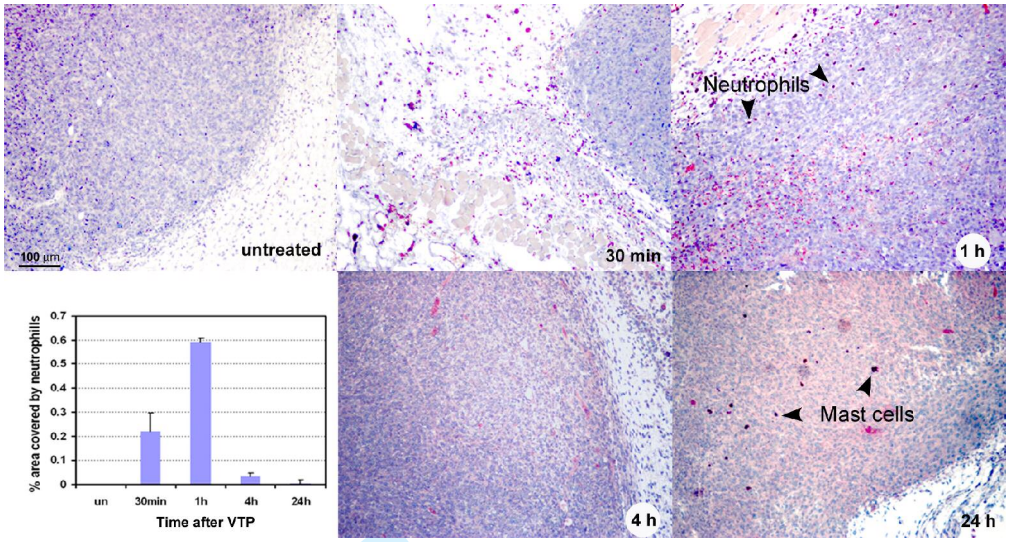
100 µm
untreated
30 min
Neutrophils
1 h
% area covered by neutrophils
0.7
0.6
0.5
0.4
0.3
0.2
0.1
0
un
30min
1h
4h
24h
Time after VTP
4 h
Mast cells
24 h

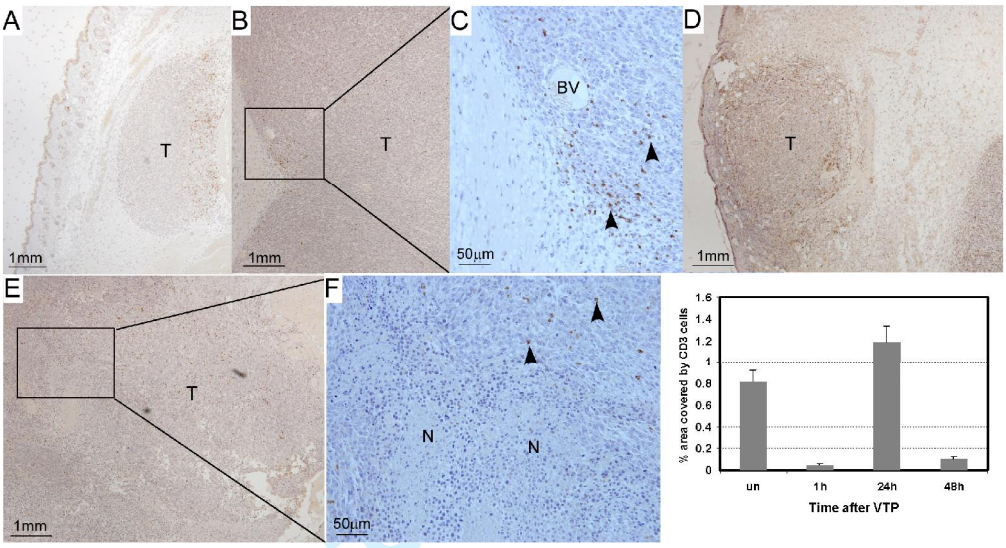

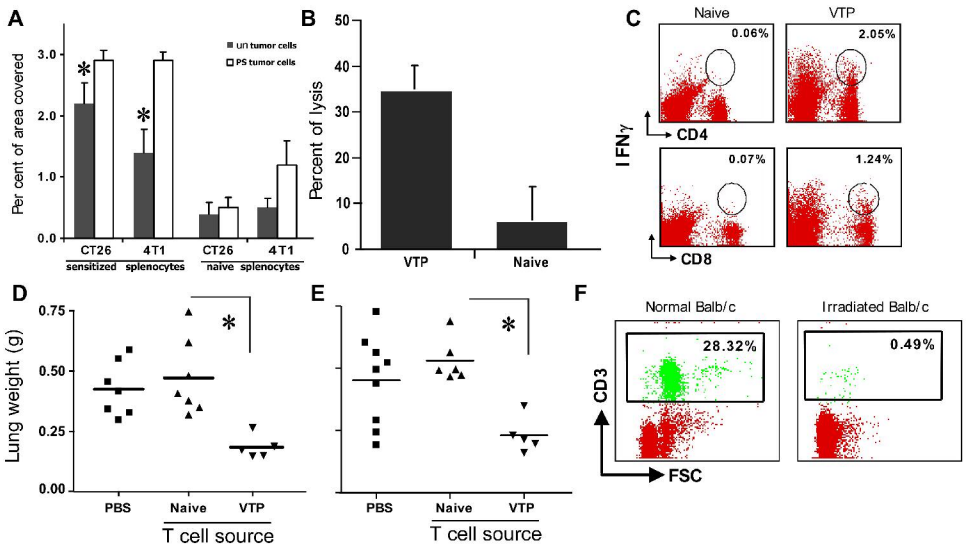

Figure 5
177x182mm (600 x 600 DPI)

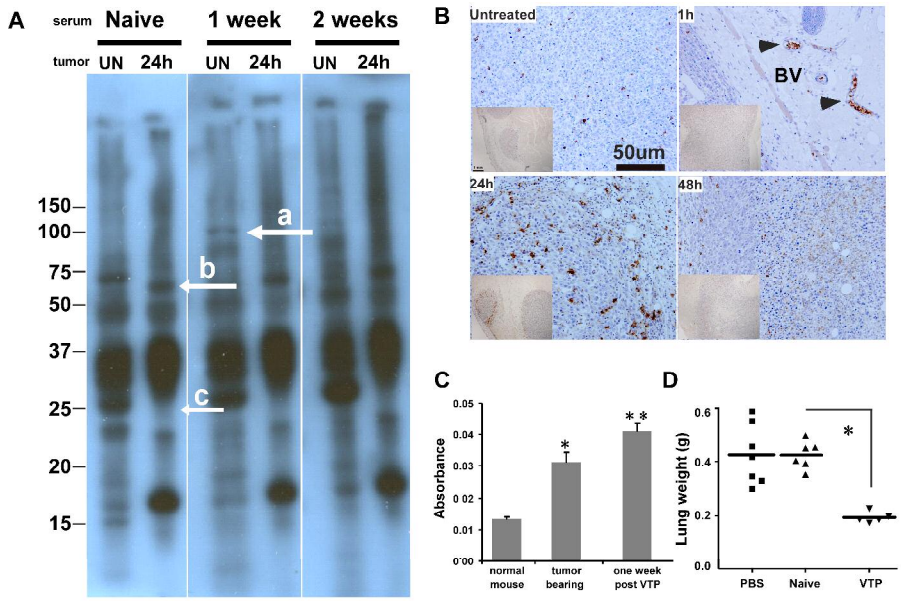

Figure 6
196x118mm (600 x 600 DPI)

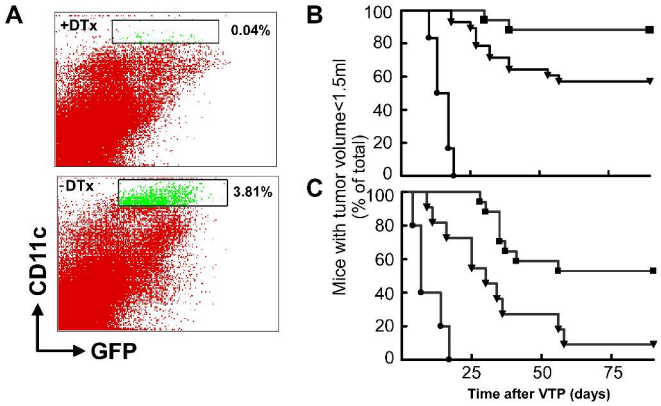

202x188mm (600 x 600 DPI)